


# Cr and CrO<sub>x</sub> etching using SF<sub>6</sub> and O<sub>2</sub> plasma

Cite as: J. Vac. Sci. Technol. B 39, 032201 (2021); doi: 10.1116/6.0000922

Submitted: 16 March 2021 · Accepted: 16 March 2021 ·

Published Online: 7 April 2021



Vy Thi Hoang Nguyen,<sup>1</sup>  Flemming Jensen,<sup>1</sup> Jörg Hübner,<sup>1</sup> Evgeniy Shkondin,<sup>1</sup>  Roy Cork,<sup>1</sup> Kechun Ma,<sup>2</sup> Pele Leussink,<sup>3</sup> Wim De Malsche,<sup>4</sup> and Henri Jansen<sup>1,a)</sup>

## AFFILIATIONS

<sup>1</sup>DTU Nanolab, Technical University of Denmark, 2800 Kgs. Lyngby, Denmark

<sup>2</sup>MicroCreate B.V., 7535 CH Enschede, Netherlands

<sup>3</sup>Mesa+ Nanolab, University of Twente, 7522 NB Enschede, Netherlands

<sup>4</sup>μflow Group, Vrije Universiteit Brussel, Pleinlaan 2, Brussels 1050, Belgium

<sup>a)</sup>Electronic mail: [henrija@dtu.dk](mailto:henrija@dtu.dk)

## ABSTRACT

Chromium is a frequently encountered material in modern nanofabrication, directly as a functional material (e.g., photomask generation) or indirectly as a hard mask (e.g., to etch quartz). With the continuous downscaling of devices, the control of the feature size of patterned Cr and CrO<sub>x</sub> becomes increasingly important. Cr and CrO<sub>x</sub> etching is typically performed using chlorine–oxygen-based plasma chemistries, but the nanoscale imposes limitations. In this work, directional etching is demonstrated for the first time using fluorine–oxygen-based plasma. Two cases are studied to demonstrate the Cr etch performance: (i) a plasma mixture of SF<sub>6</sub> + O<sub>2</sub> and (ii) a switching SF<sub>6</sub>/O<sub>2</sub> procedure in which the plasmas are used sequentially. The proposed mixture performs with Cr etch rates (ERs) up to 400 nm/min at 300 W platen power and is highest when the SF<sub>6</sub>/O<sub>2</sub> gas ratio is ~0.75%, i.e., almost pure O<sub>2</sub> plasma. The profile shows reasonable directionality but the etch selectivity is low, less than 5 toward Si, due to the high generated self-bias of 420 V. The selectivity of the plasma mixture can be improved at a lower plasma power, but this is accompanied with considerable undercut. The etching of CrO<sub>x</sub> proceeds without the need for O<sub>2</sub> in the feed, and, therefore, the ER can reach much higher values (beyond 2000 nm/min at 300 W). As the plasma mixture seems to be inadequate, a sequential process is studied with improved selectivity while preserving directionality. The high selectivity is achieved by using relatively low plasma power (to ensure a low self-bias) and the directionality is due to the time separation of the SF<sub>6</sub> and O<sub>2</sub> plasmas and a controlled directional removal of CrF<sub>x</sub> etch inhibiting species. Using such a switched procedure at 30 W plasma power, a selectivity beyond 20 with good profile directionality is achieved and having an etch rate of ~1 nm per cycle (or 7 nm/min).

Published under license by AVS. <https://doi.org/10.1116/6.0000922>

## I. INTRODUCTION

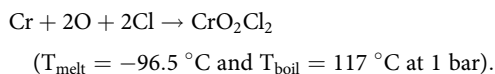
Chromium is a popular material in modern nanodevice fabrication. As a material, Cr is opaque (useful in optical lithography),<sup>1–3</sup> conductive (enabling many sensors and actuators),<sup>4–8</sup> and wear-resistant in harsh environments (useful as a hard mask in plasma etching).<sup>9–15</sup> It is also an important adhesion layer for noble metals, and it prevents dewetting (such as gold)<sup>16,17</sup> and forms a self-limiting dense and thin oxide layer that protects it from further corrosion, which is crucial in all-Cr single electron transistors devices based on Cr/CrO<sub>x</sub>/Cr junctions.<sup>18,19</sup> Other potential applications lay in photonic crystals where the Cr layer is usually relatively thick,<sup>20</sup> RF MEMS electrodes,<sup>21,22</sup> or corrosion resistant purification membranes.<sup>23,24</sup> As the last example, the half-metallic and ferromagnetic

CrO<sub>2</sub> (known from the old-fashioned cassette tape) is currently having a revival in spin-based devices for nanomagnet arrays and bit-patterned media.<sup>25</sup>

In our previous publications, we introduced a new plasma etch sequence—called CORE—able to structure high aspect ratio (AR) features into silicon.<sup>26–28</sup> CORE stands for Clear, Oxidize, Remove, and Etch and is a room temperature process dedicated for ultrahigh AR fabrication that uses a cycle of SF<sub>6</sub> plasma to etch Si and O<sub>2</sub> to protect the sidewalls of the etching features. Cr is of particular interest in the CORE sequence as it serves as a durable hard mask in the quest to go beyond an AR of 100 in Si etching. In our latest publication, we have used the liftoff procedure to pattern Cr.<sup>28</sup> However, with the continuous downscaling of the requested nanoscale devices, the control of the feature size of patterned Cr

becomes increasingly more important, and the liftoff is neither sufficiently accurate nor reliable at the nanoscale. This is why plasma etching has become the standard technique, already for many decades, in mainstream nanofabrication.

The plasma etching of Cr is currently almost exclusively reserved for chlorine–oxygen-based chemistry by forming chromyl chloride ( $\text{CrO}_2\text{Cl}_2$ ) as the final etch product.<sup>29–41</sup> The consensus is that both chlorine (e.g.,  $\text{Cl}_2$  plasma) and oxygen radicals (e.g.,  $\text{O}_2$  plasma) are needed to create the volatile chromyl chloride product. It was demonstrated by Abe *et al.*<sup>29</sup> roughly 45 years ago and a few years later explained by Nakata *et al.*<sup>30</sup> by the reaction



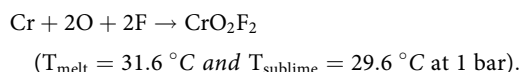
As both O and Cl radicals are needed to remove a Cr atom, possibly allowing any intermediate  $\text{CrO}_x\text{Cl}_y$  reaction path, the etch rate (ER) shows an optimum for a specific ratio between the supplied  $\text{Cl}_2$  and  $\text{O}_2$  gas. This ratio is typically around 30%  $\text{O}_2$  in the  $\text{Cl}_2 + \text{O}_2$  mixture, but depends on the temperature and other plasma parameters.<sup>33,40</sup> Indeed, at low  $\text{O}_2$  content, the formed  $\text{CrCl}_x$  species have a very high melting temperature ( $\text{CrCl}_2$  and  $\text{CrCl}_3$ ) or simply decompose ( $\text{CrCl}_4$ ). At high  $\text{O}_2$  concentrations, the  $\text{CrO}_x$  species are difficult to evaporate as well. In contrast,  $\text{CrO}_2\text{Cl}_2$  boils at  $117^\circ\text{C}$ , so in a low pressure environment (i.e., the plasma reactor) it will easily evaporate even at room temperature (Fig. 1).<sup>40</sup>

Even though Cr is typically patterned with the Cl–O-based chemistry, there are some challenges at the nanoscale. For instance,  $\text{CrO}_2\text{Cl}_2$  is an unstable compound already at about  $150^\circ\text{C}$ .<sup>35,43</sup> As a result,  $\text{CrO}_x$  species, released by the decomposition, deposit on close-by surfaces including the emerging sidewalls. Therefore, the process is getting exceedingly more difficult to pattern the smallest and/or high aspect ratio features. Furthermore, the Cl-based process is contaminating the reactor (Al corrodes heavily with  $\text{Cl}_2$  species)

and adequate cleaning and conditioning protocols are needed especially when the reactor has to be opened.<sup>31,32</sup> Another troublesome feature is the influence of the total amount of Cr (and resist)—called loading effect—on the (local) etch rate.<sup>1–3,33,36–38</sup> This will negatively affect the etch uniformity as over etching is required and profiles start to vary across the wafer and between wafers in barrel etchers.<sup>3,37,38</sup>

During this overetch, the feature sidewalls tend to straighten, but at the expense of expanding the trench size and shrinking the feature. Consequently, also the critical dimension (CD) etch performance is compromised, which hampers the minimum achievable feature size.<sup>1–3</sup> When aiming at higher aspect ratio features or thicker Cr layers, also RIE lag (the smaller gaps etch slower) will play a role.<sup>1,38,39</sup> On top of these Cr issues, the high  $\text{O}_2$  concentration erodes the photoresist (both vertically and laterally) and the selectivity (typically less than two)<sup>1,20,35,36</sup> and resist retraction<sup>1,12,34,37</sup> will restrict the CD performance. Additionally, there is a tradeoff between the requested straightness of the etch profile and mask selectivity. The reason is that during etching, one always needs a mask on top of the Cr film and there is always a substrate below the Cr film. Typically, the mask will be photoresist and the substrate Si. If one decides to increase the  $\text{O}_2/\text{Cl}_2$  ratio to improve directionality, the selectivity toward the resist will drop. Identically, if one needs to decrease the ratio, the selectivity toward the Si will drop. So, there is a compromise between profile, mask selectivity, and substrate attack. Furthermore, reactor history (or memory effect) is an important issue as it is found that Cr films are damaged (i.e., etched) even for seemingly pure oxygen plasma conditions.<sup>44,45</sup> The etching is likely caused by Cl contributions stuck on the reactor walls from a preceding etch process. Therefore, reproducibility is often a difficult task.

To fight the above challenges, alternative mixtures have been proposed such as adding reducing agents (like  $\text{CO}_2$ ,  $\text{C}_2\text{H}_5\text{OH}$ , or  $\text{H}_2$ )<sup>1,34–36</sup> or performing cryogenic etching,<sup>39,40</sup> with some encouraging results. However, in this study, we propose a drastically different approach. As many of the above issues are related to the specific chemistry, this paper will present the etch performance of Cr thin film by exchanging the chlorine by fluorine radicals. The reaction process probably resembles the established Cr–Cl–O reaction but replacing Cl by F:



So, for this reaction, O and F radicals are needed to form volatile chromyl fluoride ( $\text{CrO}_2\text{F}_2$ ). Surprisingly, the  $\text{CrO}_2\text{F}_2$  species is rarely mentioned in the literature even though its existence is known for long.<sup>42</sup> At standard room pressure, it sublimates readily at  $29.6^\circ\text{C}$  and melts at  $31.6^\circ\text{C}$  (Fig. 1 taken from Ref. 42). In other words, Cr should be easily patterned at a sufficiently low process pressure when the substrate holder is kept at room temperature. To test this behavior, an experimental procedure has been designed with patterned and as-deposited Cr and  $\text{CrO}_x$  thin film.

## II. MATERIALS AND METHODS

The procedure to study the etch performance of Cr and its oxide in F–O-based plasma will use both patterned and nonpatterned coated wafers. The nonpatterned wafers are simply used

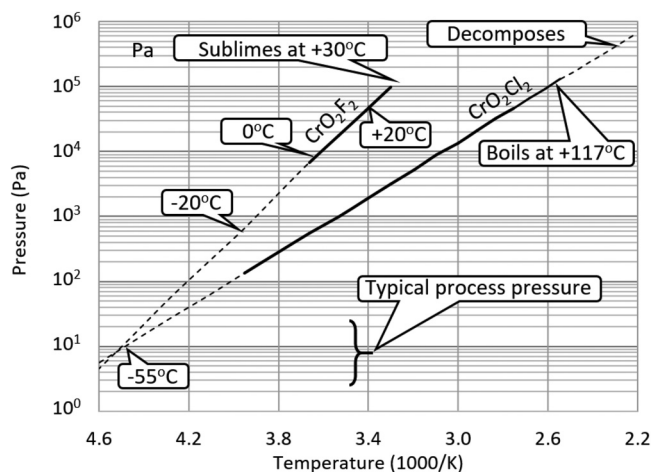


**FIG. 1.** Vapor pressure of  $\text{CrO}_2\text{Cl}_2$  and  $\text{CrO}_2\text{F}_2$ . The solid line part is data reproduced from Refs. 40 and 42. The estimated extrapolated sublimation temperature at 76 mT is  $-55^\circ\text{C}$  and presented by the dashed lines.

to find some quick indication on overall etch rate (ER) performance without considering the selectivity or profile. With this information, patterned samples will be etched using promising plasma settings and analyzed with SEM to extract the profile and selectivity toward Si.

**Nonpatterned samples:**  $\langle 100 \rangle$  Si wafers (150 mm diameter) are prepared with 70 nm Cr (Lesker CMS18 sputter system). The Cr-coated wafers are cleaved into  $2 \times 1 \text{ cm}^2$  chips and individually mounted in the center of a 150 mm diameter Si carrier wafer using a tiny drop of Galden® PFPE fluid (Solvay Solexis SpA) for sufficient thermal contact or only to fix it. In addition,  $\text{CrO}_x$  coated wafers are created having 30 nm Cr with 200 nm  $\text{CrO}_x$  on top using reactive sputtering. The as-deposited  $\text{CrO}_x$  layer has a refractive index of 2.39, which is close to the expected 2.55 value for  $\text{Cr}_2\text{O}_3$ . These Cr/ $\text{CrO}_x$  samples are prepared using a sputter tool (PRO Line PVD75, Kurt J. Lesker). Cr is sputtered from a Cr target at 3 mTorr pressure and 350 W DC power. The deposition rate of 0.33 nm/s is measured by profilometry (Dektak XTA stylus profiler, Bruker).  $\text{CrO}_x$  is deposited in the same chamber and from the same target using reactive DC sputtering with oxygen. Ar and  $\text{O}_2$  flows are set to 50 and 10 sccm, respectively, while the pressure and power are the same as in Cr sputter deposition. The deposition rate (0.08 nm/s) and optical functions are determined by ellipsometry (VASE, J.A. Woollam).

**Patterned samples:** Si wafers are prepared with (i) a single sputter run of 70 nm Cr and 30 nm polySi or (ii) 1000 nm evaporated Cr and 150 nm sputtered polySi. Cr is deposited using an e-beam system (Temescal FC2000, Ferrotec) and the deposition rate is fixed at 1 nm/s. The wafer is transferred to the sputter system (PRO Line PVD75, Kurt J. Lesker) where poly-silicon is deposited at 3 mTorr pressure and 120 W RF power. The deposition rate of 0.031 nm/s is determined by ellipsometry. The wafers are receiving a layer of 65 nm BARC (DUV42S-6) and 360 nm DUV resist (KRF 230Y) using a spin coating system (Gamma 2M spin-coater, Süss MicroTech). Subsequently, line patterns (200 nm wide, 400 nm pitch) are defined by a DUV stepper (FPA-3000EX4, Canon) equipped with a 248 nm KrF excimer laser. The exposure dose is  $86 \text{ mJ/cm}^2$ . Then, the wafers are developed in 2.38% tetra-methyl-ammonium-hydroxide in water (AZ726 MIF, AZ Electronic Materials), rinsed in de-ionized water, and spin dried with a gentle nitrogen stream. Again, the patterned wafers are cleaved into  $1 \times 1 \text{ cm}^2$  chips and mounted on an Si carrier wafer.

**Etching:** the prepared samples are loaded into a commercial dual source etch system (SPTS/Pegasus DRIE). The dual source plasma can provide ICP assisted etching, but in this study, the RIE mode is used (i.e., solely platen power).<sup>28</sup> The system has been dedicated for  $\text{SF}_6/\text{O}_2$  based plasma etching only and has no prior fluorocarbon or chlorine history. The FC- and Cl-free chamber is needed to ensure the absence of any contamination or influence that might affect the Cr etch performance. In the case of blanket samples, the ER is simply deduced by continuing etching until the Cr (or  $\text{CrO}_x$ ) is gone and dividing the 70 nm (or 200 nm) by the recorded time. In the case of patterned samples, prior to the Cr etch, first the 65 nm BARC layer is etched using  $\text{O}_2$  plasma followed by a polySi etch using switching  $\text{SF}_6/\text{O}_2$  plasma to open the Cr surface to be etched. The initial Cr etch setting is fixed at 200 sccm total flow at 2% throttle valve ( $\rightarrow \sim 60 \text{ mT}$ ) and 100 W platen power (between 270 and  $140 V_{dc}$  bias). The  $\text{SF}_6$  flow is

varied to extract the influence of the  $\text{SF}_6/\text{O}_2$  ratio (i.e., %  $\text{SF}_6$ ) on the ER for four temperatures:  $-20$ ,  $0$ ,  $20$ , and  $40 \text{ }^\circ\text{C}$ .

**Analysis:** after the etching, the Galden heat transfer fluid is wiped gently from the backside of the patterned samples with alcohol sprayed on a tissue and the sample is cleaved manually using a diamond pen for SEM analysis (Supra V60, Zeiss).

### III. RESULTS AND DISCUSSION

In this section, first the blanket Cr and  $\text{CrO}_x$  samples will be investigated using the  $\text{SF}_6 + \text{O}_2$  plasma mixture. This will lead to a proposed Cr etch mechanism quite similar to the Cl-O-based chemistry. After this, the patterned samples will be studied using the preferred condition from the blanket etches. Finally, the process is optimized for nanoscale pattern transfer by replacing the plasma mixture by a switching  $\text{SF}_6/\text{O}_2$  plasma sequence.

#### A. Nonpatterned samples etched in $\text{SF}_6 + \text{O}_2$ plasma mixtures

##### 1. Effect of $\text{SF}_6/\text{O}_2$ ratio on the Cr etch rate

The initial etches using the blanket Cr samples are presented in Fig. 2. Just like the Cl-O-based Cr etching, the F-O-based chemistry shows a pronounced optimum indicating that indeed both F- and O-species are needed to chemically etch the Cr layer. Both pure  $\text{O}_2$  plasma and pure  $\text{SF}_6$  plasma will barely etch as the products are not volatile. Furthermore, as the ER is close to zero for pure  $\text{O}_2$ , where the  $V_{dc}$  is around 270 V, the influence of pure physical etching (i.e., sputtering) can be ignored. Also, for both chemistries, the ER increases for higher temperatures. But, unlike the Cl-O-based chemistry where the maximum ER is typically found around 70–80%  $\text{Cl}_2$  of the total flow, the  $\text{SF}_6 + \text{O}_2$  peaks below 1%  $\text{SF}_6$ . Another remarkable difference between the two chemistries is that for the Cl-O-based chemistry, the ER at the lower  $\text{Cl}_2$  concentrations (less than 70%) is depending on temperature. This is in contrast with the F-O-based chemistry where the  $\text{SF}_6$  concentrations below 0.25% seem to show minimal temperature dependency above  $0 \text{ }^\circ\text{C}$ . Furthermore, at these lower concentrations, the ER seems to depend linearly on the %  $\text{SF}_6$  in the feed.

The above result suggests that the process for lower  $\text{SF}_6/\text{O}_2$  ratios is plasma-supply limited and that surface reactions are fast enough to have no effect on the ER. This preliminary conclusion needs a closer look. Therefore, an additional control experiment is performed to confirm the temperature independency. Carefully selected samples having the same area (to prevent loading to affect the ER) and taken from adjacent parts of a broken blanket Cr-coated wafer (to ensure the same Cr thickness), are etched with a 0.25%  $\text{SF}_6$  feed (i.e., nicely into the presumed plasma-supply limited region). The same recipe is used three times at  $-20 \text{ }^\circ\text{C}$  and the same for  $0$ ,  $20$ , and  $40 \text{ }^\circ\text{C}$ . So, a total of 12 samples are going to be etched that should show an identical result. To ensure a conclusion with sufficient confidence, some indication of possible error is needed as described next. The control experiment is going to be performed with a total flow of 200 sccm, so we apply  $0.25\% = 0.5 \text{ sccm SF}_6$ . The  $\text{SF}_6$  uses a 50 sccm  $\text{N}_2$ -calibrated mass flow controller (SFC5400, Sensirion) having an accuracy of 2% and repeatability of 0.2% full scale. The thermal conversion factor for  $\text{SF}_6$  is 0.26. Therefore, the actual full scale is 13 sccm. So, the requested

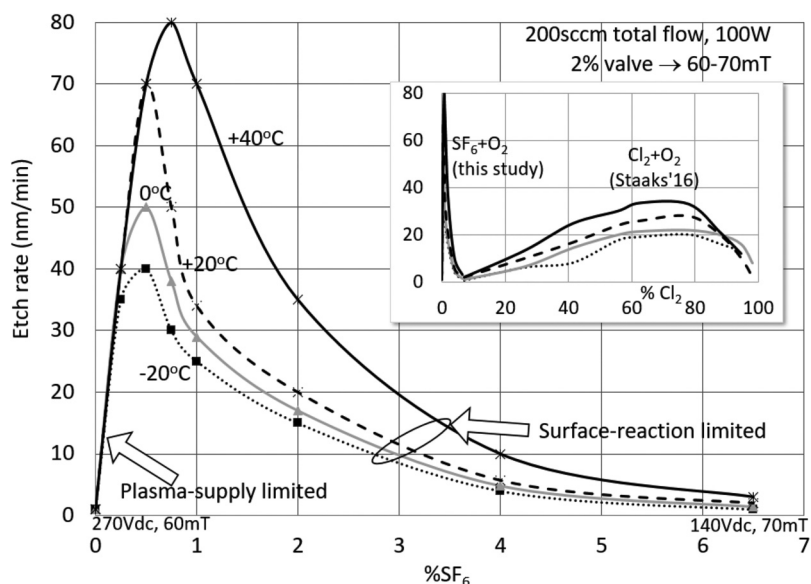


**FIG. 2.** Cr etch rate as a function of the  $\text{SF}_6/\text{O}_2$  ratio for  $-20$ ,  $0$ ,  $20$ , and  $40$  °C. The inset compares the Cr ER with  $\text{Cl}_2 + \text{O}_2$  plasma. The latter is reproduced data taken from Ref. 36.

0.5 sccm  $\text{SF}_6$  has an accuracy of 0.26 sccm and repeatability of 0.026 sccm. As we perform identical etches during the same day (so drift is low), only the repeatability is important for the error analysis. In other words, the flow for all the twelve etches will be within 0.026 sccm. The error for the vertical axis (the ER) is found by identifying accurately the time needed to clear the Cr layer. Note that as we have taken identical chips from adjacent broken wafer locations, we might misjudge the actual ER, but relatively the thickness has no influence. So, only the actual time to clear the Cr layer should be determined accurately. The adopted procedure has been to first etch a sample for 120 s and—after substrate unload—confirming optically that the Cr is gone (because the ER is  $\sim 40$  nm/min and we have  $\sim 70$  nm Cr). Subsequently, another sample is etched for 100 s to confirm that the Cr is still present. The result has been that all the control samples between 0 and 40 °C etch faster than  $70/2 = 35$  nm/min, but slower than  $70/1.66 = 42$  nm/min. The three samples etched at  $-20$  °C are all between 32 and 35 nm/min. So, it is confirmed that the reproducibility of the ER of all the samples is within 10% and we are confident that the conclusion of a temperature-independent process at the lower %  $\text{SF}_6$  content is correct.

## 2. Effect of plasma power and gas flux on the Cr etch rate

Now, it has been deduced that the ER at lower  $\text{SF}_6/\text{O}_2$  concentration is limited by the supply of active species from the plasma bulk and not the reaction speed at the Cr surface, the next question is what controls the supply. Here are two main influences, the plasma power and the flux of species (i.e., pressure and/or flow). Which one contributes most and when is tested by varying both the plasma power and total flux in a reasonable broad process window, but for a fixed temperature (40 °C),  $\text{SF}_6/\text{O}_2$  ratio (0.5%), and exposed Cr surface area ( $2 \text{ cm}^2$ ). Initially, the throttle valve is fixed too at 2%, which means that the pressure increases when extra gas is added.

As expected, Fig. 3 shows that the ER increases when the total flow [Fig. 3(a)] or power [Fig. 3(b)] is increased. However, for 50 W plasma power, the ER barely increases between 100 and 800 sccm. Seemingly, all the available power is converted above 100 sccm and extra gas will not enhance the ER. Similarly, in Fig. 3(b), the ER for 100 sccm tends to saturate at higher power. Now, the amount of gas is controlling the ER and extra power will not help. Interestingly, the ER doubles if both the power and the flow are doubled. This is indicated by the dashed lines in Fig. 3(a). For example, the ER for 800 sccm at 200 W is twice the ER for 400 sccm at 100 W and quadruple the ER for 200 sccm at 50 W.

However, the flux of active species depends on both the process pressure and gas flow and in Fig. 3 the throttle valve has been fixed, so the process pressure increased together with the flow. To find out which one of these variables affects the ER most, pressure or flow, an additional experiment is needed to separate these two contributions. This time, instead of fixing the turbo throttle valve, the pressure is fixed and the throttle is allowed to adapt for the different applied gas flows. Figure 4(a) presents how the ER depends on the process pressure for different fixed gas flows: 200, 400, and 800 sccm. As the curves for 200, 400, and 800 sccm almost coincide, we conclude that the pressure and not the flow controls the ER in the process window investigated. Seemingly, only little of the incoming gas supports Cr etching and the rest leaves the reactor unused. So, a more appropriate conclusion of the previous finding is that the ER doubles when both the power and the pressure are doubled (and not the flow). Furthermore, the indicated self-bias solely depends on the pressure and the flow has a minor effect [Fig. 4(b)].

## 3. Effect of $\text{SF}_6/\text{O}_2$ ratio on the Cr and $\text{CrO}_x$ etch rate

With the information of the optimum parameter settings, the graph of Fig. 2 is partly repeated to get a more detailed curve for low  $\text{SF}_6/\text{O}_2$  ratios at 40 °C, but this time including  $\text{CrO}_x$  and at the



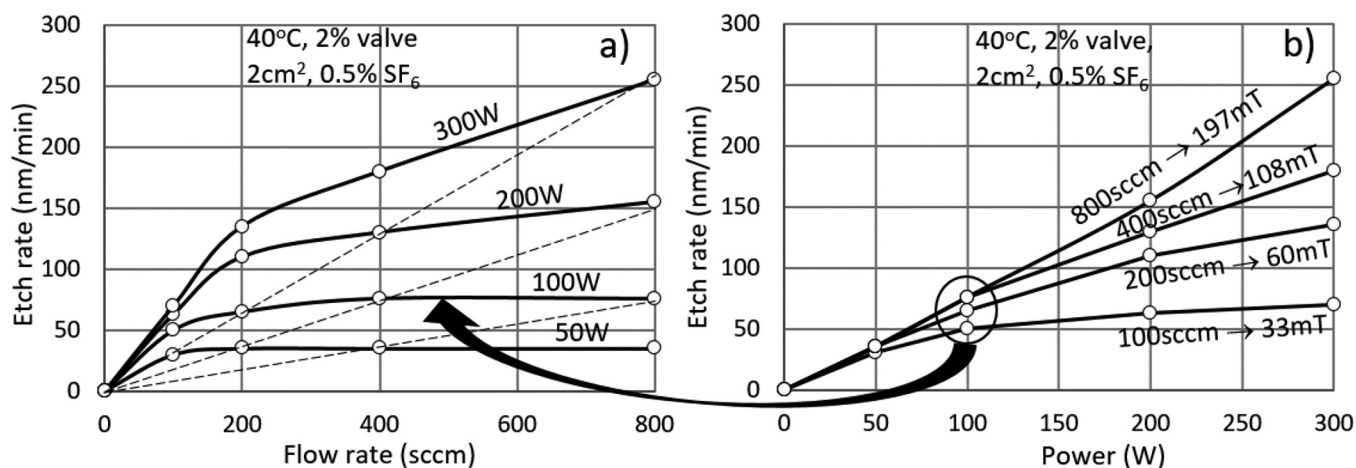
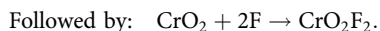
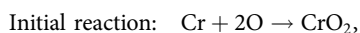


**FIG. 3.** Cr ER for different varying total gas flow at 2% fixed throttle (a) and plasma power (b). The temperature is fixed at 40 °C and the exposed area is always 2 cm<sup>2</sup>. The SF<sub>6</sub>/O<sub>2</sub> ratio is kept at 0.5%.

highest allowed power (300 W), pressure (200 mT), and temperature (+40 °C). The ER is plotted in Fig. 5(a) for Cr and CrO<sub>x</sub> as a function of the %SF<sub>6</sub> concentration at 800 sccm total flow. As before, at very low SF<sub>6</sub>/O<sub>2</sub> ratios the Cr ER increases linearly with the %SF<sub>6</sub> in the feed and around 0.5% the increase in ER slows down. The ER peaks at ~0.75% SF<sub>6</sub> in the oxygen feed gas and then drops. In contrast, the CrO<sub>x</sub> ER continues to increase with added SF<sub>6</sub>. Figure 5(b) allows some different plasma settings and higher SF<sub>6</sub>/O<sub>2</sub> ratios. It shows that the CrO<sub>x</sub> ER increases until it saturates just below 2500 nm/min. The saturation is caused by the limited pressure and power supply: there is simply not sufficient supply (either energy or gas) to support a higher ER. Also for the CrO<sub>x</sub>, the highest pressure shows the highest ER that barely depends on the flow.

#### 4. Proposed Cr etch mechanism in the SF<sub>6</sub> + O<sub>2</sub> plasma mixture

The above findings bring us to the most likely surface reactions taking place in the F–O chemistry:



Starting from pure O<sub>2</sub> plasma that creates O radicals, the Cr surface rapidly oxidizes and forms a protective skin that prevents further oxidation. Then, by introducing small amounts of SF<sub>6</sub>, F radicals will react with adsorbed CrO<sub>x</sub> species and form volatile chromyl fluoride. This departure will expose fresh Cr that will immediately react with the plenty of available O radicals and the volatile reaction awaits the next F radical to arrive. The latter process will go faster—and thus the ER increases—when more SF<sub>6</sub> is added. The ER will improve further with an extra supply of SF<sub>6</sub> until F radicals start to attach to the exposed Cr layer before O radicals arrive. If this happens, part of the exposed Cr is going to be fluorinated producing a nonvolatile CrF<sub>x</sub> layer that will block the

spontaneous reaction and the ER will go down. The CrF<sub>x</sub> shielding will continue until around 6% SF<sub>6</sub> in the SF<sub>6</sub> + O<sub>2</sub> feed, the ER becomes virtually zero when the whole surface becomes fluorinated. For the CrO<sub>x</sub> material, the situation is different as the Cr is already fully oxidized. Therefore, the ER continues to increase with additional SF<sub>6</sub> without showing an optimum ER because the protective CrF<sub>x</sub> skin cannot be created. It will saturate though when the power or flux (being it pressure or flow) is insufficient to create additional radicals. As the CrO<sub>x</sub> ER continues to increase with extra SF<sub>6</sub>, while the Cr ER drops to virtually zero, the selectivity at higher SF<sub>6</sub>/O<sub>2</sub> ratios will go to very high values (>>10 000). This observation implies that it is possible to accurately remove a CrO<sub>x</sub> surface layer of a Cr thin film by exposing the surface to a pure SF<sub>6</sub> plasma. The F radicals will first create volatile CrO<sub>2</sub>F<sub>2</sub> and then seal the Cr surface with CrF<sub>x</sub>. It also implies that any interstitial CrO<sub>x</sub> in a Cr thin film (e.g., the polycrystalline boundaries) might be attacked even in low bias pure SF<sub>6</sub> plasma and potentially may create pinholes and exposing the underlying (Si) material.

The somewhat complex ER behavior of Cr is not unusual in plasma etching in general. For instance, in Si etching using SF<sub>6</sub> + O<sub>2</sub> mixtures, it is also found that when the plasma power is relatively high and the flux is low, the flux will follow the radical production: the flux-controlled (or power-saturated) region. In contrast, if the flux is sufficiently high and the power is low, the power will control the ER: the power-controlled (or flux-saturated) region.<sup>46</sup> Also, for Si etching, the ER doubles when both the power and flux are doubled, but in contrast, in Si etching the flow and not the pressure determines the ER.<sup>46</sup> The authors do not know why, but maybe the depletion of active species plays a crucial role.

#### 5. Cr loading effect

A specific observation is that the ER found in Fig. 5 is higher than that expected from Fig. 3 at 300 W. This is because the samples selected for this experiment were smaller in area (but also this time they are all

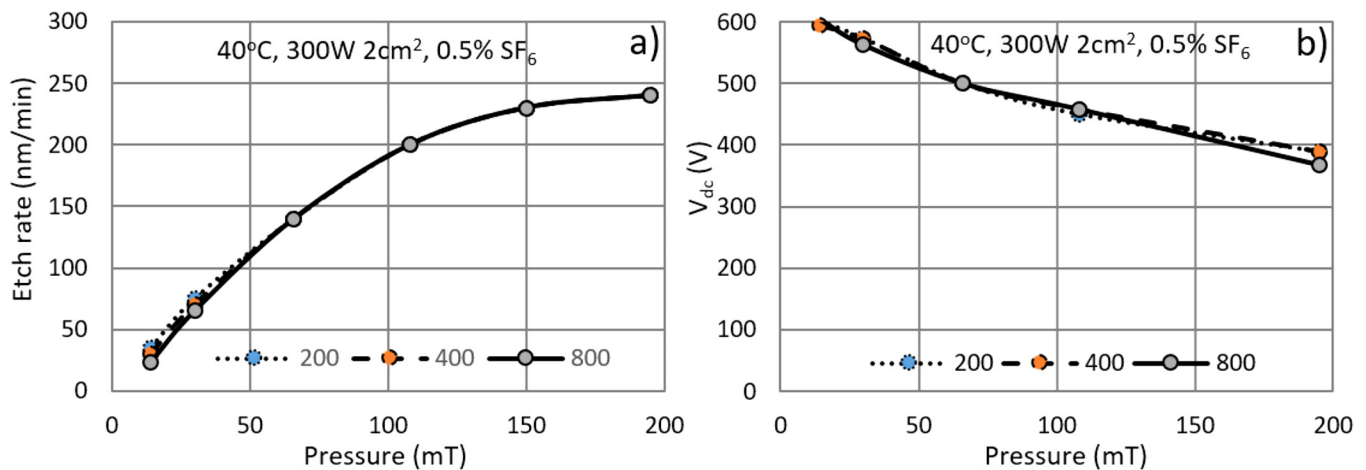


FIG. 4. Cr ER (a) and self-bias (b) as a function of pressure for 200, 400, and 800 sccm total flow.

identical within the experiment). This brings us to the subject of how the loading affects the ER. Mogab was the first to derive an equation, which correctly predicts the loading effect.<sup>47</sup> The loading effect is the decrease in ER for an increasing area of etching material inside the plasma. In a simplistic manner, one could argue that the amount of etched material will not change for an identical plasma setting, and therefore, the ER drops 2 times when the exposed area is doubled.

A more detailed and more correct analysis though can be found in a paper on Si etching by the authors where also a pragmatic loading equation is formulated,<sup>46</sup>

$$ER = ER_{sat} / (1 + \alpha L) \quad ER_{sat} = 525 \text{ nm/min} \quad \alpha = 0.25 \text{ cm}^{-2}$$

at 300 W, 200 mT, 40 °C.

The saturation etch rate  $ER_{sat}$  occurs for very low Cr loading area  $L$  and  $\alpha = \alpha(T)$  is a constant depending on the lifetime of the etching species and thus temperature.<sup>32,47</sup> Both  $ER_{sat}$  and  $\alpha$  are varying with the specific plasma setting and can be deduced by measuring a few ER values for different  $L$  values. For example, as presented in Fig. 6, for a sample of  $1.5 \text{ cm}^2$  etched at 300 W and 200 mT, we find  $ER = 380 \text{ nm/min}$ ; for  $3 \text{ cm}^2$ , it is  $300 \text{ nm/min}$ ; and for  $6 \text{ cm}^2$ , we find it to be  $210 \text{ nm/min}$ . Therefore,  $ER_{sat} = 525 \text{ nm/min}$  and  $\alpha = 0.25 \text{ cm}^{-2}$ . So, only when  $\alpha L \gg 1$ , i.e.,  $L > 20 \text{ cm}^2$ , the above simplistic “1/L” rule holds. Furthermore, the samples have been placed on an Si carrier. Seemingly, this carrier does not affect the F concentration, even though  $\text{SiF}_4$  is very volatile. This indicates that there is a passivating  $\text{SiO}_2$  layer present that prevents consumption.

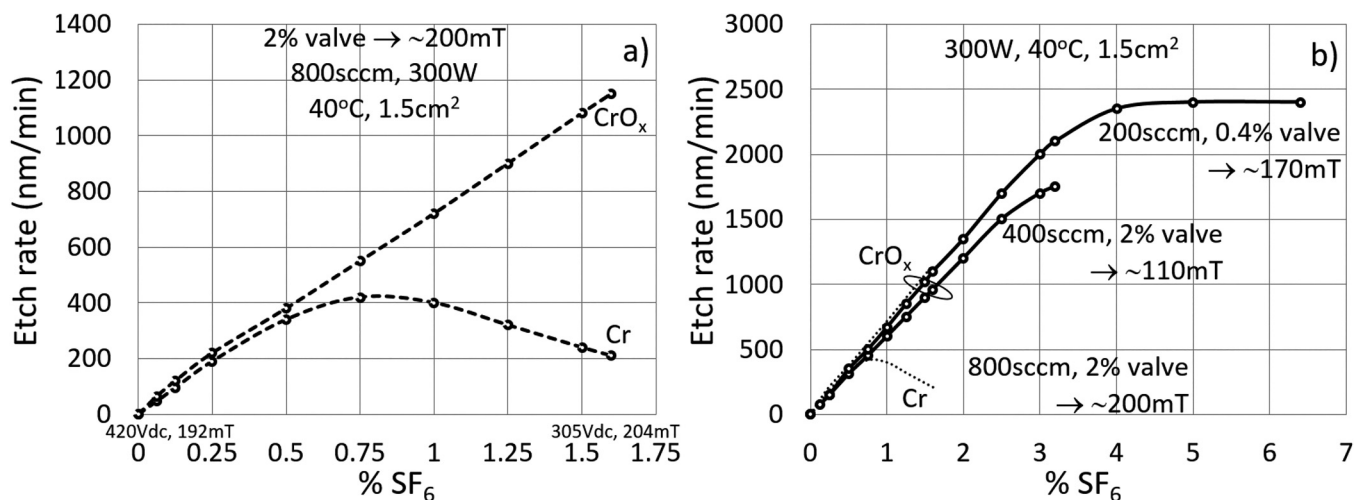
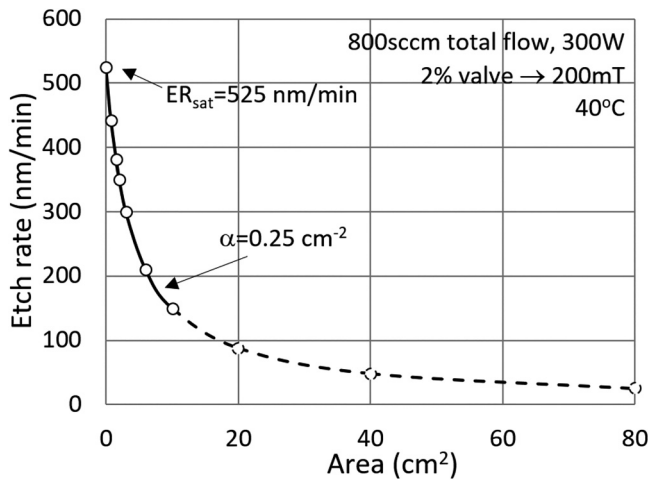


FIG. 5. Cr (a) and  $\text{CrO}_x$  (b) ER as function of %  $\text{SF}_6$  at fixed 300 W,  $A = 1.5 \text{ cm}^2$ , and  $40 \text{ }^\circ\text{C}$ .



**FIG. 6.** Cr ER as a function of loading at fixed 300 W, 800 sccm total flow, and 40 °C.

### B. Patterned Cr samples etched in mixed SF<sub>6</sub> + O<sub>2</sub> plasma

Having established a much faster etch rate than usual in Cl-based plasmas, the next topic to discuss is the etch profile and selectivity for the F-based chemistry. The first remark is that the almost pure O<sub>2</sub> concentration of the F-O-based chemistry needed to etch Cr means that photoresist will etch very fast and consequently the selectivity is rather low. Therefore, an intermediate hard mask is needed to transfer a resist pattern reliably. We have opted for polySi as this material is standard available and perfectly compatible with mainstream fabrication processes. An even stronger argument though is that Si will virtually not etch in pure O<sub>2</sub> due to the strong oxidation into nonvolatile SiO<sub>2</sub> products. This means that both the polySi mask and bulk Si underneath the Cr layer will be preserved during the Cr etch and we do not have to settle for a compromise. Furthermore, polySi can be etched with

extreme high selectivity toward resist and Cr using established F-based plasmas<sup>46-49</sup> of course as long as the bias is not too high to dominate the ER.

Initial etches were performed using a mixed plasma close to the optimized ER setting from Fig. 5 with 0.5% SF<sub>6</sub>/O<sub>2</sub> ratio, 200 sccm total flow, and 150 mT. As expected and observed in Figs. 7 and 8, the patterned Cr ER increases for higher power and higher temperature settings and having the tendency to saturate. Furthermore, it is measured that the polySi ER scales quadratic with the plasma power (as both the ion density and ion energy increase with power) and does not depend on the temperature. This is a strong indication that the Si is eroded physically, probably using an intermediate formation of SiO<sub>2</sub>. As a consequence, the etch selectivity increases quickly when the plasma power is reduced. The odd pronounced sideways cut into the Cr approximately halfway through the layer (indicated by the arrow →) is believed to be caused by rapid CrO<sub>x</sub> removal. This layer seems to have developed during the Cr deposition, which has been performed in two evaporation runs even though the vacuum has not been broken in between.

### C. Patterned Cr samples etched in switched SF<sub>6</sub>/O<sub>2</sub> plasma

The most important observation in the mixed process is that it seems to be hard to have both a directional profile and at the same time a reasonable etch selectivity. Furthermore, the selectivity increases strongly when the power is lower and the temperature high enough to support spontaneous chemical etching (i.e., above 20 °C). The same type of difficulty arises during room temperature Si etching using a mixture of SF<sub>6</sub> on O<sub>2</sub>. As a major improvement on the latter mixed processes, recently the authors demonstrated excellent directional and selective performance of the switched CORE procedure.<sup>26-28</sup> Therefore, the same switched procedure has been tested for Cr etching. First, an important parameter to minimize is the plasma power as we learned from the mixed process that the etch rate of Si quickly drops (and thus the selectivity increases) when the power is lowered. We have chosen 30 W. Furthermore, the Cr etch is accomplished by switching the chemistry back-and-forth between an oxygen-rich

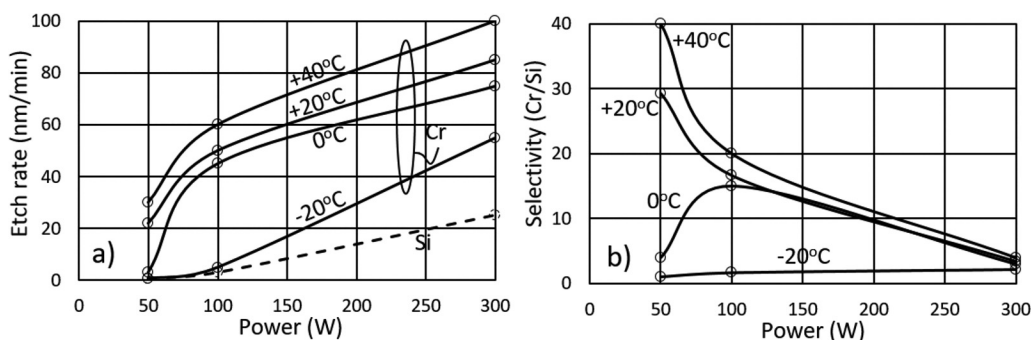


**FIG. 7.** Patterned Cr ER (a) and etch selectivity (b) toward Si as a function of plasma power for different temperatures at 0.5% SF<sub>6</sub>/O<sub>2</sub> ratio, 200 sccm total flow, and 150 mT. The Si ER is 0.75 nm/min at 50 W (45 Vdc), 3 nm/min at 100 W (140 Vdc), and 25 nm/min at 300 W (420 Vdc).

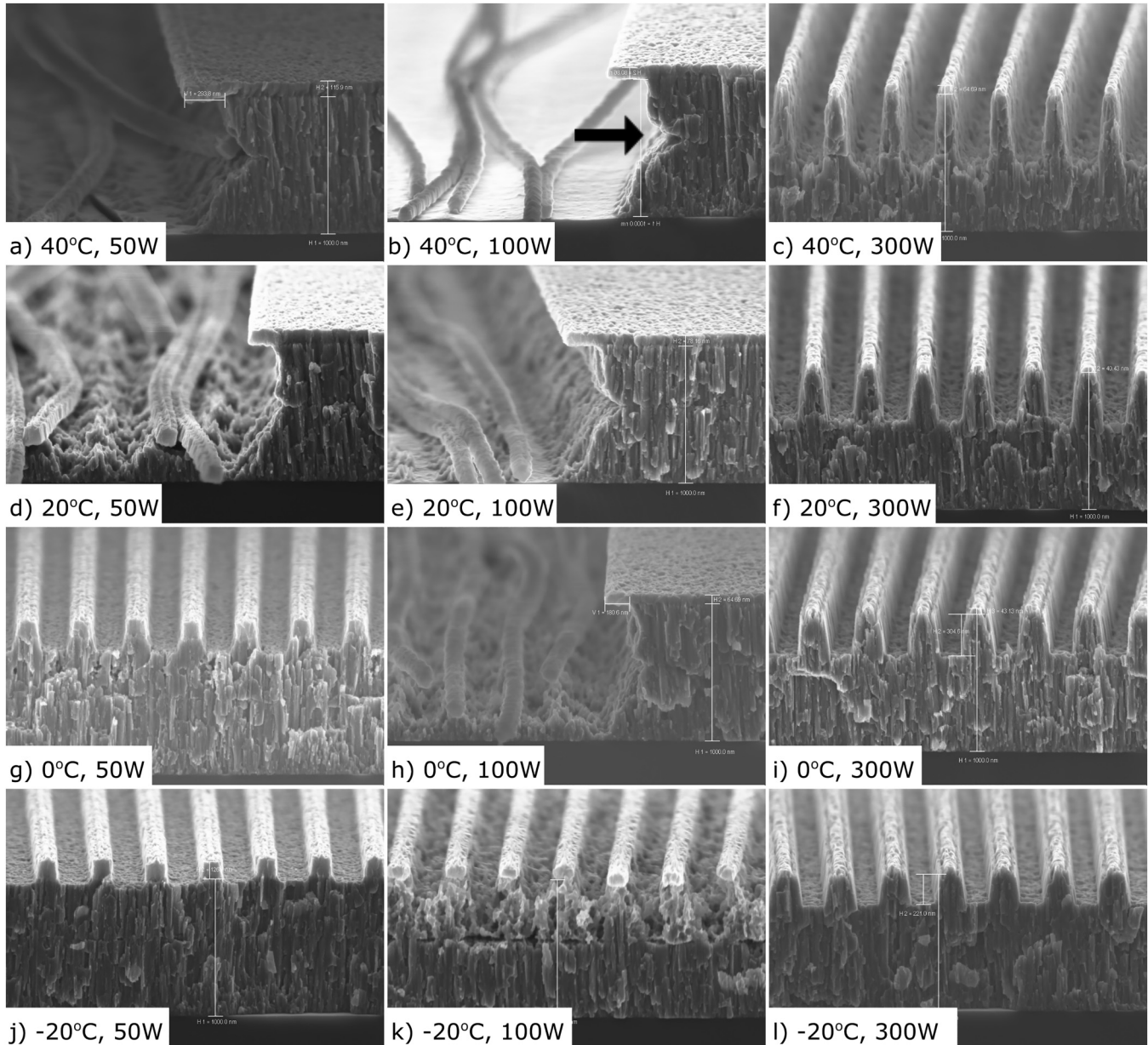


**FIG. 8.** Cr etch using mixed 0.5% SF<sub>6</sub> in O<sub>2</sub> plasma for various temperature and plasma power. The mask is 150 nm polySi on top of 1000 nm Cr. The etch time is 40 min at 50 W, 20 min at 100 W, and 4 min at 300 W. The patterned Cr ER increases for higher power and higher temperature settings and having the tendency to saturate. The Si ER is not depending on temperature and scales approximately quadratic with plasma power.

(O-step) and fluorine-rich (F-step) plasma. To be precise, the O-step uses 50 sccm pure O<sub>2</sub> and takes 9 s. The F-step uses 50 sccm O<sub>2</sub> + 3 sccm SF<sub>6</sub> for 1 s (=6% SF<sub>6</sub>/O<sub>2</sub> ratio). The latter might sound O-rich, but is already far in the regime where F radicals start to dominate the surface coverage (see Fig. 2). Both steps are performed at 20 °C, 50 mT, and 30 W power (70 Vdc). In the F-step, it is opted to keep the O<sub>2</sub> flowing to prevent major plasma

changes that might trigger the matching unit to change and causing etch fluctuations. Nevertheless, if matching is not an issue, switching between pure O<sub>2</sub> and pure SF<sub>6</sub> might turn out to be favorable. Further research is needed though.

Figure 9 shows a slightly positive tapered etch of 350 nm into the Cr with the polySi mask still present (116 nm left, so an etch selectivity of ~10). The sidewall barely shows an undercut, which



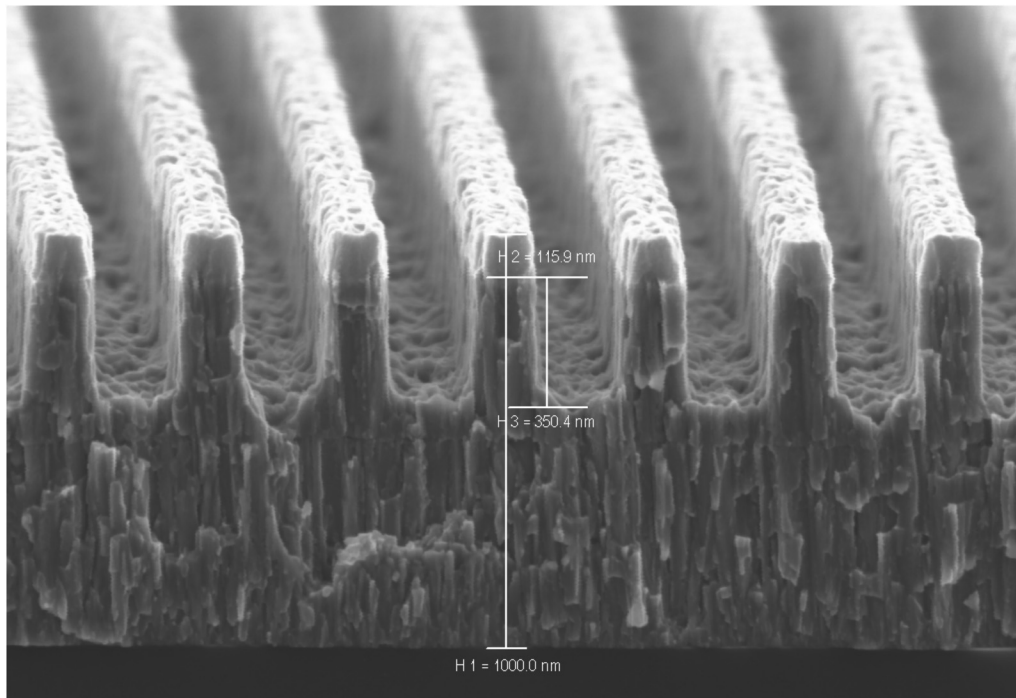


**FIG. 9.** Cr etch for 45 min of 1000 nm thick Cr lines by switching the chemistry back-and-forth between an oxygen-rich (9 s O-step using 50 sccm  $O_2$ ) and fluorine-rich (1 s F-step using 50 sccm  $O_2$  + 3 sccm  $SF_6$ ) plasma operating at 30 W platen power and 50 mT. The lines are etched beyond 300 nm with good selectivity toward the initial 150 nm polySi mask. The chaotically arranged vertical lines are a result of the polycrystalline film growth during Cr deposition.

indicates a protective layer being present. This layer cannot be  $CrO_x$ , because such a layer will always be converted into volatile  $CrO_2F_2$  species during the  $SF_6$  step and causing an undercut. Therefore, seemingly the only candidate is  $CrF_x$ . This means that  $CrF_x$  presumably does not react spontaneously with O radicals into volatile  $CrO_2F_2$ . As the  $CrF_x$  covered sidewall is without ion bombardment, the O radicals cannot reach the Cr and undercutting is prevented. In contrast, the bottom surface receives a constant supply of ions that removes F-species (or  $CF_x$ ) and O radicals can attach. Subsequently, the  $CrO_x$  layer is removed by F radicals and etching proceeds directionally.

Clearly, the switched procedure shows a much better etch performance compared to the mixed process albeit showing a much lower etch rate. The latter is not a disadvantage though as we are requesting nanoscale accuracy anyways. The etch depth after 45 min of etching (i.e., 270 cycles) is around 330 nm. This means that  $\sim 1.2$  nm Cr is removed per step. This indicates that the etch process might enable atomic layer etching (ALE). The reason is explained with the help of Fig. 10. Assume initially that the Cr layer is pristine and single crystalline [Fig. 10(a)]. When  $O_2$  plasma is provided, the surface will rapidly oxidize and self-limit after a thin  $CrO_x$  layer is formed that blocks further oxidation [Fig. 10(b)]. The next  $SF_6$  plasma will create F radicals that spontaneously react with the  $CrO_x$  species and form volatile  $CrO_2F_2$  [Fig. 10(c)]. After the  $CrO_x$  has been removed, the F radicals will fluorinate the

surface and form again a passivating film, but this time it is  $CrF_x$  that blocks further fluorination [Fig. 10(d)]. So, also this layer is assumed to be self-limiting. Only by ionic (and directional) impact, this layer can be removed (defluorinated) after which the Cr surface is pristine again [Fig. 10(e)]. The cycle is now ready for the next oxidation step [Fig. 10(f)]. It is now easy to understand why the switched Cr etch procedure is superior to the mixed process. The selectivity is higher because most steps do not acquire ionic bombardment. Only the defluorination step in Fig. 10(e) needs ions to remove the  $CF_x$  blocking film.

As explained, ideally in the model from Fig. 10, only one layer of Cr will be removed per cycle. The lattice constant of Cr is 0.3 nm, so we should have found an ER of 0.3 nm per cycle. However, the experimental number is 1.2 nm (or four layers) per cycle and this number is also not fixed. This difference is likely because we have ignored the following phenomena. (i) The additional ER due to physical bombardment has been ignored, but the generated self-bias (70 Vdc) is a bit high. Therefore, it is possible that in Fig. 10(e) not just F will leave but rather  $CrF_x$ . This would already double the ER per cycle. In fact, the  $V_{dc}$  is always present, so the oxidation step might also remove the additional material. (ii) In addition, it is observed that the as-deposited surface of the polycrystalline Cr is very rough and this contributes to the ER as the exposed surface is more than if the surface would have been perfectly flat and smooth. (iii) Furthermore, the ER might be

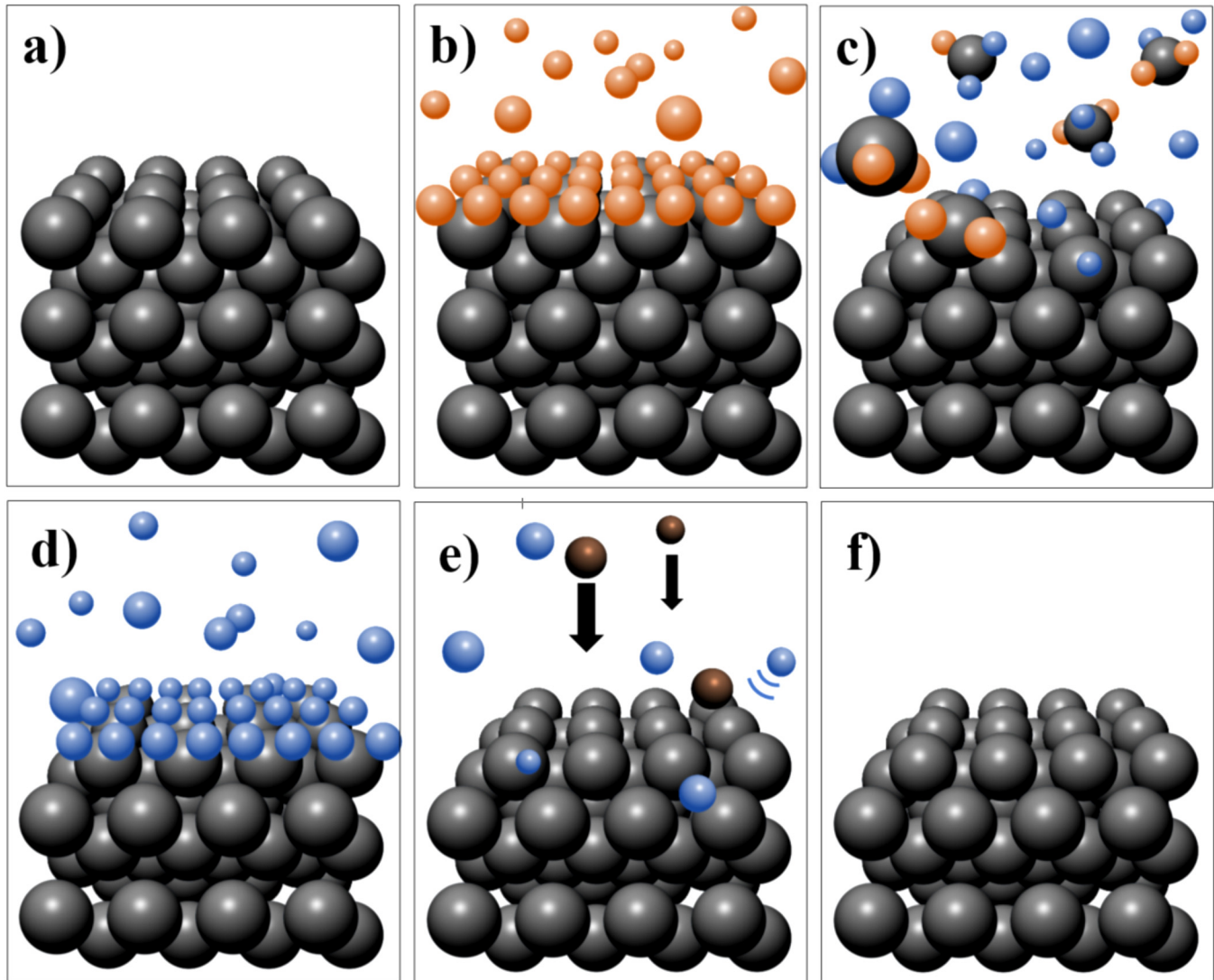


**FIG. 10.** Proposed etch model for Cr etching using a cycle of  $O_2$  and  $SF_6$  plasma. Pristine Cr (a) is exposed to O radicals (b). The  $CrO_x$  is removed with F radicals forming  $CrO_2F_2$  (c) and will leave the surface fluorinated (d). The  $CrF_x$  is sputtered by ion impact (e) and is ready for the next cycle (f).

higher because the plasma has to pass the ER peak back-and-forth (Fig. 2). This cannot proceed instantaneously and thus compromises the process transient and will add some ER due the passing peak observed in Fig. 2. (iv) Then, it is neither obvious nor proven that the oxidation or fluorination process limits to exactly one monolayer. The same issue occurs for the regrowth of native oxide.<sup>26</sup> (v) Finally, the deposited Cr is neither a pure nor a single crystalline. Cr is a well-known getter material and easily takes up residual oxygen and water molecules during evaporation or sputtering. In particular, subsurface O-contamination may greatly affect the final result as we already noticed that F radicals effectively convert  $CrO_x$  species into volatile  $CrO_2F_2$ . Altogether, it

should not be a surprise to find a higher ER than allowed for ALE. To come closer to the ideal ALE process, further study is needed, e.g., we might lower the self-bias substantially to prevent physical sputtering (e.g., by use of the ICP source) or start with a perfectly smooth Cr material (i.e., buy single crystal chromium wafers or  $CrF_3$  wafers and test if it indeed does not react with oxygen plasma).<sup>50</sup>

Now that a convenient Cr etch procedure has been defined, it is worthwhile to see how it operates in a complete fabrication scheme of Si nanostructures using photoresist as a mask. Figure 11(a) shows the initial 400 nm pitch DUV grating pattern on top of the stack of layers to be etched. The stack is composed of 70 nm Cr + 30 nm

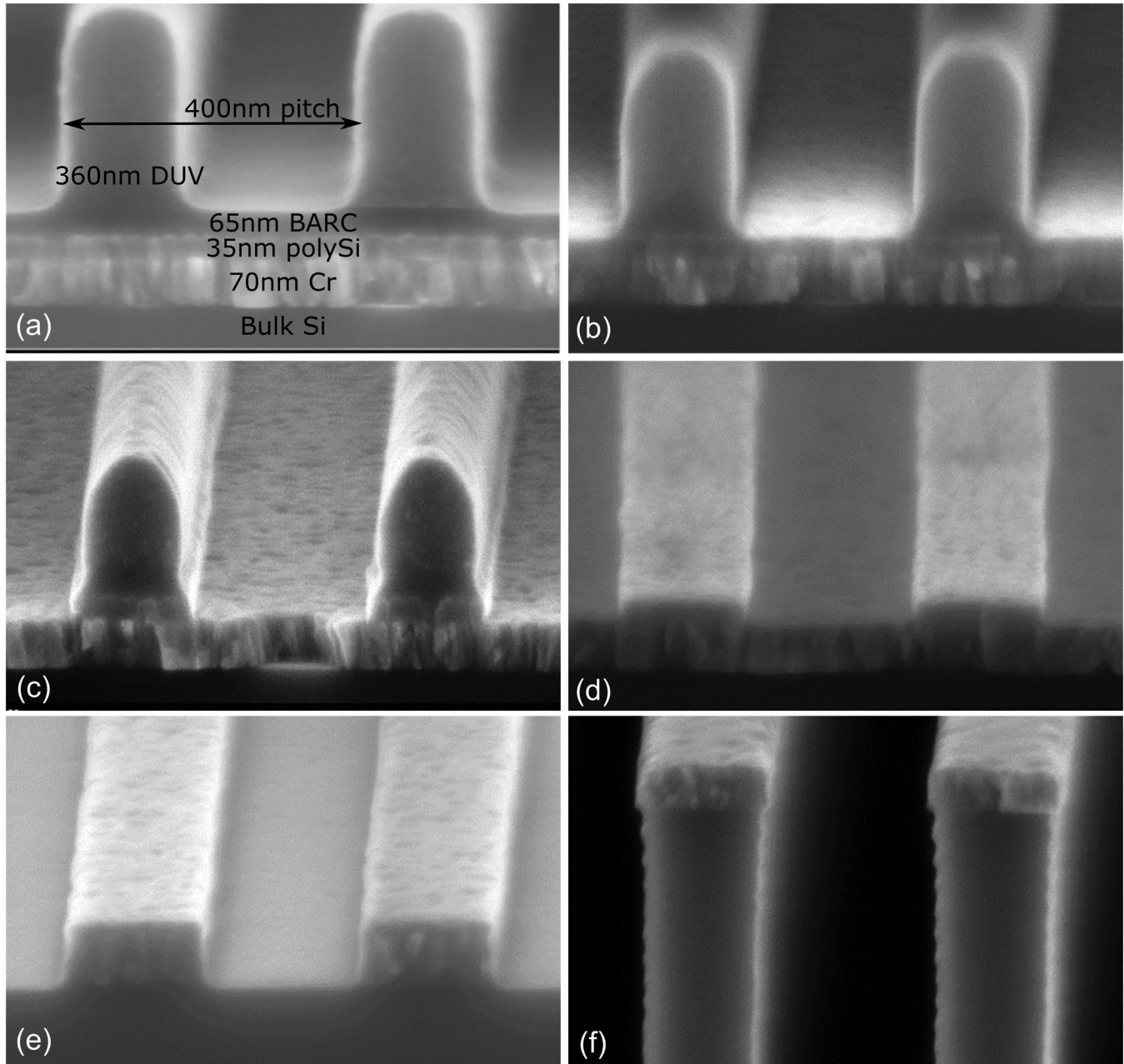


**FIG. 11.** Etch procedure of a 400 nm pitch grating pattern composed of 360 nm thick DUV resist on top of the sample stack: bulk Si + 70 nm Cr + 30 nm polySi + 65 nm Barc. The sample is etched without braking vacuum in the same system in a single run: (a) the initial measures before the etch, (b) after O-based directional Barc etch, (c) directional polySi etch using the switched SF<sub>6</sub>/O<sub>2</sub> CORE sequence, (d) isotropic polymer strip, (e) directional Cr etch, and (f) the final transfer into the bulk Si.

polySi + 65 nm Barc. First, the Barc polymer is etched using 50 sccm O<sub>2</sub> plasma for 10 min [Fig. 11(b)]. The throttle valve is fully opened (100%) to ensure a low process pressure (~1 mT) that will promote ions to control the pattern transfer (radicals will cause undesirable mask retraction).<sup>12</sup> The plasma power is kept low at 10 W (showing

18 Vdc) to minimize the physical impact of ionic species that would degrade the pattern shape. Subsequently, the polySi is etched using ten cycles of the CORE sequence as formulated in a previous paper [Fig. 11(c)].<sup>28</sup> This etch is followed by a 10 min O<sub>2</sub> plasma resist strip [Fig. 11(d)]. This step is performed at sufficiently high pressure



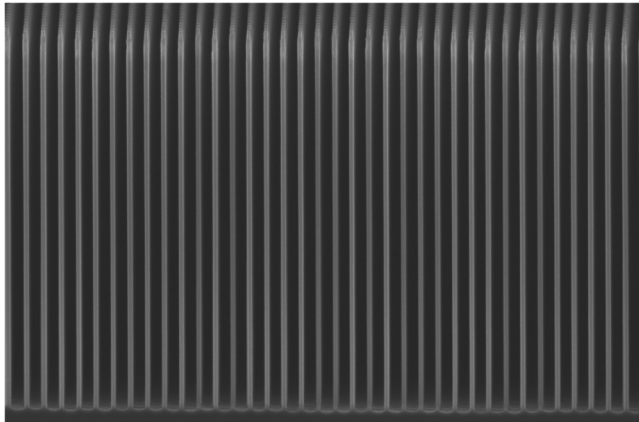


**FIG. 12.** Zoom-out of Fig. 11(f) after a prolonged etch time ( $9\mu\text{m}$  deep). The Cr mask is just gone.

(50 mT) to promote radical etching in favor of an ion-enhanced process to prevent any surface damage. Subsequently, the Cr is etched using the F–O-based switching chemistry [Fig. 11(e)]. Finally, the patterned Cr mask is used to etch the bulk Si using the CORE sequence [Fig. 11(f)].

Figure 12 is a zoom-out from Fig. 11(f) of the etched Si bulk using the patterned Cr for a  $9\mu\text{m}$  deep grating pattern. Clearly, the pattern transfer proceeds with high fidelity and the 70 nm Cr layer allows an AR beyond 50. However, while etch time proceeds, the Cr mask shows pronounced retraction that restricts the maximum achievable AR as already observed in our previous paper.<sup>28</sup> Figure 13 shows how the Cr mask slowly erodes not only normally but also laterally. The latter is problematic as it will degrade the topside of the nanoscale features after prolonged etch time. This side erosion is of course the consequence of using both O- and F-generating gases for the Si etching. This is true even when etching is performed in a sequence where both plasmas are not present at the same time (i.e., a switching cycle). After all, in agreement with the findings reported in this paper, during the

O-step of the CORE sequence, the Cr surface will oxidize and self-limit. However, this  $\text{CrO}_x$  layer will be removed in the subsequent F-step of the cycle and thus removes some Cr. This is specifically true when additional bias is provided (i.e., the R-step of the CORE sequence). In the next cycle, this “monolayer” Cr removal will happen once more. It should be noted though that the CORE sequence is operating most of the cycle time in the pure  $\text{SF}_6$  regime. It is, therefore, rational to believe that the Cr will be highly fluorinated and only occasionally some of the Cr will be oxidized and removed as chromyl fluoride. It is of course the quest of the CORE sequence to limit this type of mask erosion as much as possible.

#### IV. CONCLUSION

In this study, a novel directional Cr etch technique is presented based on a mixture or sequence of  $\text{SF}_6$  and  $\text{O}_2$  plasma. Just like the Cl-based chemistry, which needs O and Cl radicals to etch Cr by forming volatile chromyl chloride ( $\text{CrO}_2\text{Cl}_2$ ), the F-version is explained by considering a binary process that needs both O and F radicals to proceed by forming volatile chromyl fluoride ( $\text{CrO}_2\text{F}_2$ ). Unlike  $\text{CrO}_2\text{Cl}_2$ , which is known to decompose easily at temperatures well below  $150^\circ\text{C}$  thereby forming nonvolatile  $\text{CrO}_x$  products,  $\text{CrO}_2\text{F}_2$  sublimates readily at room temperature presumably leaving the surface clean. Also, by omitting Cl species (and C in case  $\text{CCl}_4$  plasma is used), the reactor stays clean, corrosion-free and process drift is believed to be minimized even though the long-term etch behavior of this novel technique is yet unknown. The supply of  $\text{O}_2$  during Cr etching means that an intermediate hard mask is needed as the photoresist is rapidly eroded. We have opted for (poly-) silicon due to its compatibility and straightforward implementation in mainstream nanofabrication.

The  $\text{SF}_6$  and  $\text{O}_2$  plasma combination is shown to have some favorable characteristics with respect to the conventional approach using  $\text{Cl}_2$  and  $\text{O}_2$  plasma. The observed etch directionality is explained by considering the formation of volatile chromyl fluoride ( $\text{CrO}_2\text{F}_2$ ) in which the Cr is first reacting with O radicals into  $\text{CrO}_x$  and subsequently reacts with F radicals into  $\text{CrO}_2\text{F}_2$ . The complementary reaction of Cr first reacting with F radicals into  $\text{CrF}_x$  and then with O radicals into  $\text{CrO}_2\text{F}_2$  presumably does not

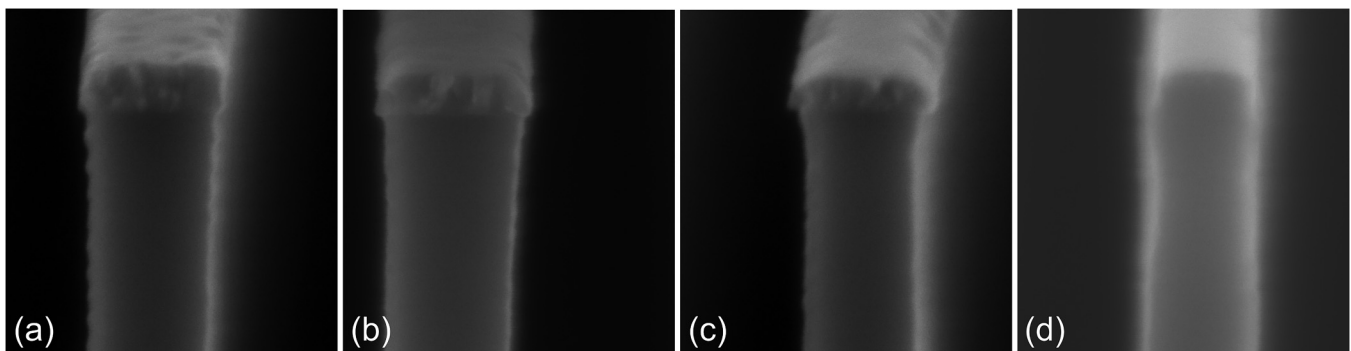


**FIG. 13.** Mask retraction during  $\text{SF}_6\text{-O}_2$  plasma etching of bulk silicon: (a) after 1 h  $\rightarrow 1.4\mu\text{m}$ , (b) 2 h  $\rightarrow 2.5\mu\text{m}$ , (c) 4 h  $\rightarrow 4.2\mu\text{m}$ , and (d) 8 h  $\rightarrow 6.8\mu\text{m}$  deep Si etch.



occur or is of minor importance. The directionality is thus explained by considering that the sidewall will be protected by  $\text{CrF}_x$  species. Only the application of ionic impact will rupture this layer on the bottom surfaces and etching continues in a straight fashion. Two different Cr etch procedures are studied. The first technique is based on mixing a small amount of  $\text{SF}_6$  (1% or less) with  $\text{O}_2$ . The second technique is much like the procedure used in ALE in which a time-multiplexed procedure is performed where both gases are introduced sequentially.

With respect to ER, the mixed F-chemistry compares favorably with conventional Cl-based etching albeit pronounced mask undercutting. The ER of Cr is  $\sim 10$  times faster at fairly identical power conditions. The selectivity toward photoresist is for many cases insufficient, because the etching is performed in almost pure  $\text{O}_2$  plasma. However, for the same reason, the selectivity toward Si is high, much higher than possible in Cl-based Cr etching. Therefore, the use of polySi as a mask is demonstrated and promoted. Furthermore, the mixed F–O-plasma can sculpture  $\text{CrO}_x$  isotropically with even higher ER. An ER beyond 2000 nm/min is reached at 300 W plasma power, which is approximately 100 times faster than typical in Cl-based plasma.

Even though the mixture is beneficial for microscale etching (e.g., to create a thick Cr hard mask useful in glass plasma etching), for nanofabrication, a high selectivity and low undercut are preferred. Therefore, the switched procedure is introduced. It shows excellent nanoscale characteristics. A selectivity of 20 is achievable with virtually no undercut (zero CD loss) at a controllable low ER. So, due to the small  $\text{SF}_6/\text{O}_2$  gas ratio, the Si ER is low and the resulting selectivity toward the Cr is high. This is in big contrast with conventional Cl-based Cr etching where the selectivity seldom exceeds 2 and the ER rarely tops 30 nm/min. A high selectivity is valuable in order to get the highly appreciated “zero CD process bias” in optical photomask generation using MoSi-based phase-shift masks. Furthermore, this F/O switch cycle is a candidate to demonstrate ALE as both F and O steps are presumably self-limiting and, therefore, the ER will depend on the number of cycles and less on the length of the individual steps. For this reason, the ER should be addressed in nm per cycle rather than in nm per minute. The ALE condition is only true of course when the bias is sufficiently high to remove the  $\text{CrF}_x$  surface layer, but low enough not to encourage physical sputtering of the underlying bulk Cr.

Even though the initial results of F–O-based etching of Cr have shown some very promising results, questions remain and should be addressed in future work. For instance, the switching sequence is not at all perfect. The plasma does not allow the gases to be replaced instantaneously. This means that there will be a transition period where the plasma passes through the “0.75%” peak and both fluorine and oxygen radicals will act together. This will surely promote undercut. To prevent this from happening, one could introduce additional steps in between both steps. This is like the CORE sequence where the C-step has been introduced to prevent fluorine from the E-step to compete with the oxygen radicals needed in the O-step. Also, the addition of oxygen in the F-step might need to be replaced by, e.g., argon in order to push the Cr etch system as far as possible into the pure F-based chemistry. Furthermore, the current self-bias of 70 Vdc is relatively high and limits the selectivity between Cr and Si. So, by no means, the

current recipes are optimized and improvements are foreseen. In particular, the addition of large amounts of  $\text{O}_2$  in the F-rich step of the switch cycle needs a closer look. Nevertheless, the authors hope that the current information is sufficient and will encourage others to give the F–O chemistry to etch Cr a try.

## ACKNOWLEDGMENTS

The authors would like to thank the DTU Nanolab staff for instrument support. In particular, they thank Matthias Keil for support with DUV lithography and Roy Cork and Martin Nørvang Kristensen for the technical support with plasma etching processes.

## DATA AVAILABILITY

The data that support the findings of this study are available within the article.

## REFERENCES

- 1 B. Wu, *J. Vac. Sci. Technol. B* **24**, 1 (2006).
- 2 T. Faure *et al.*, *Proc. SPIE* **7122**, 712209 (2008).
- 3 M. Hashimoto, H. Iwashita, A. Kominato, H. Shishido, M. Ushida, and H. Mitsui, *Proc. SPIE* **7028**, 702804 (2008).
- 4 V. Mulloni, *Chromium: Environmental, Medical, and Materials Studies (Chemical Engineering Methods and Technology)*, (Nova Science Publishers Inc., Hauppauge, NY, 2011).
- 5 W. J. Arora, A. J. Nichol, H. I. Smith, and G. Barbastathis, *Appl. Phys. Lett.* **88**, 053108 (2006).
- 6 Z. Peng, X. Yuan, J. C. Hwang, D. Forehand, and C. L. Goldsmith, *2006 Asia-Pacific Microwave Conference*, Yokohama, Japan, 12–15 December 2006 (IEEE, Piscataway, NJ, 2006), pp. 1535–1538.
- 7 I. Sinno, A. Sanz-Velasco, S. Kang, H. Jansen, E. Olsson, P. Enoksson, and K. Svensson, *J. Micromech. Microeng.* **20**, 095031 (2010).
- 8 M. de Boer, H. Jansen, and M. Elwenspoek, *Proceedings of the 8th International Conference on Solid-State Sensors and Actuators, Eurosensors IX*, Stockholm, Sweden, 25–9 June 1995 (IEEE, Piscataway, NJ, 1995), Vol. 1, pp. 565–568.
- 9 L. Tang, S. Y. Su, and T. Yoshie, *Proc. SPIE* **7946**, 79460M (2011).
- 10 M. N. Hossain, J. Justice, P. Lovera, B. McCarthy, A. O’Riordan, and B. Corbett, *Nanotechnology* **25**, 355301 (2014).
- 11 Z. Liu, X. Gu, J. Hwu, S. Sassolini, and D. L. Olynick, *Nanotechnology* **25**, 285301 (2014).
- 12 Y. Zhao, H. Jansen, M. De Boer, E. Berenschot, D. Bouwes, M. Girones, J. Huskens, and N. Tas, *J. Micromech. Microeng.* **20**, 095022 (2010).
- 13 H. V. Jansen, M. J. de Boer, K. Ma, M. Girones, S. Unnikrishnan, M. C. Louwerse, and M. C. Elwenspoek, *J. Micromech. Microeng.* **20**, 075027 (2010).
- 14 H. Wensink, H. V. Jansen, J. W. Berenschot, and M. C. Elwenspoek, *J. Micromech. Microeng.* **10**, 175 (2000).
- 15 H. Jansen, M. de Boer, J. Burger, R. Legtenberg, and M. Elwenspoek, *Microelectron. Eng.* **27**, 475 (1995).
- 16 X. Zhu *et al.*, *Appl. Surf. Sci.* **453**, 365 (2018).
- 17 A. B. Fanta, M. Todeschini, A. Burrows, H. Jansen, C. D. Damsgaard, H. Alimadadi, and J. B. Wagner, *Mater. Charact.* **139**, 452 (2018).
- 18 L. S. Kuzmin, Y. A. Pashkin, A. N. Tavkhelidze, F. J. Ahlers, T. Weimann, D. Quenter, and J. Niemeyer, *Appl. Phys. Lett.* **68**, 2902 (1996).
- 19 T. Kubota, and R. Yagi, *AIP Conf. Proc.* **850**, 1419 (2006).
- 20 A. P. Milenin, C. Jamois, R. B. Wehrspohn, and M. Reiche, *Microelectron. Eng.* **77**, 139 (2005).
- 21 L. J. Fernandez, E. Visser, J. Sese, R. Wiegink, J. Flokstra, H. Jansen, and M. Elwenspoek, *Sensors, 2003 IEEE*, Toronto, Canada, October 2003 (IEEE, Piscataway, NJ, 2003), Vol. 1, pp. 549–552.

- <sup>22</sup>X. Rottenberg, H. Jansen, P. Fiorini, W. De Raedt, and H. A. C. Tilmans, *2002 32nd European Microwave Conference*, Milan, Italy, September 2002 (IEEE, Piscataway, NJ, 2002), pp. 1–4.
- <sup>23</sup>H. D. Tong, F. C. Gielens, J. G. Gardeniers, H. V. Jansen, C. J. M. Van Rijn, M. C. Elwenspoek, and W. Nijdam, *Ind. Eng. Chem. Res.* **43**, 4182 (2004).
- <sup>24</sup>H. T. Hoang, H. D. Tong, F. C. Gielens, H. V. Jansen, and M. C. Elwenspoek, *Mater. Lett.* **58**, 525 (2004).
- <sup>25</sup>Q. Zhang, Y. Li, A. V. Nurmikko, G. X. Miao, G. Xiao, and A. Gupta, *J. Appl. Phys.* **96**, 7527 (2004).
- <sup>26</sup>V. T. H. Nguyen *et al.*, *ECS J. Solid State Sci. Technol.* **9**, 024002 (2020).
- <sup>27</sup>V. T. H. Nguyen, F. Jensen, J. Hubner, P. Leussink, and H. Jansen, *J. Vac. Sci. Technol. A* **38**, 043004 (2020).
- <sup>28</sup>V. T. H. Nguyen, E. Shkondin, F. Jensen, J. Hubner, P. Leussink, and H. Jansen, *J. Vac. Sci. Technol. A* **38**, 053002 (2020).
- <sup>29</sup>H. Abe, K. Nishioka, S. Tamura, and A. Nishimoto, *Jpn. J. Appl. Phys.* **15**, 25 (1976).
- <sup>30</sup>H. Nakata, K. Nishioka, and H. Abe, *J. Vac. Sci. Technol.* **17**, 1351 (1980).
- <sup>31</sup>D. L. Flamm and V. M. Donnelly, *Plasma Chem. Plasma Process.* **1**, 317 (1981).
- <sup>32</sup>J. W. Coburn, *Plasma Chem. Plasma Process.* **2**, 1 (1982).
- <sup>33</sup>H. M. Naguib, R. A. Bond, and H. J. Poley, *Vacuum* **33**, 285 (1983).
- <sup>34</sup>Y. Suzuki, T. Yamazaki, and H. Nakata, *Jpn. J. Appl. Phys.* **21**, 1328 (1982).
- <sup>35</sup>E. Hoshino, U.S. patent 4,613,401 (U.S. Patent and Trademark Office, Washington, DC, 1986).
- <sup>36</sup>S. Aoyama, S. Sakamoto, T. Koike, N. Yoshioka, N. Harashima, A. Hayashi, and T. Sasaki, *Proc. SPIE* **3748**, 137–146 (1999).
- <sup>37</sup>T. Ichiki, S. Takayanagi, and Y. Horiike, *J. Electrochem. Soc.* **147**, 4289 (2000).
- <sup>38</sup>B. Wu, J. Chen, E. Markovitz, G. Xiao, S. Tam, A. Kumar, I. Ibrahim, and W. F. Yau, *Proc. SPIE* **5992**, 59920P (2005).
- <sup>39</sup>H. Jansen, M. de Boer, R. Wiegerink, N. Tas, E. Smulders, C. Neagu, and M. Elwenspoek, *Microelectron. Eng.* **35**, 45 (1997).
- <sup>40</sup>D. Staaks, X. Yang, K. Y. Lee, S. D. Dhuey, S. Sassolini, I. W. Rangelow, and D. L. Olynick, *Nanotechnology* **27**, 415302 (2016).
- <sup>41</sup>D. Staaks, Z. Yu, S. D. Dhuey, S. Sassolini, K. Y. Lee, I. W. Rangelow, and D. L. Olynick, *J. Vac. Sci. Technol. A* **37**, 061306 (2019).
- <sup>42</sup>A. Engelbrecht and A. V. Grosse, *J. Am. Chem. Soc.* **74**, 5262 (1952).
- <sup>43</sup>S. Z. Makarov and A. A. Vakhrushev, *Bull. Acad. Sci. USSR* **9**, 1613 (1960).
- <sup>44</sup>J. Tonotani, S. I. Ohmi, and H. Iwai, *Jpn. J. Appl. Phys.* **44**, 114 (2005).
- <sup>45</sup>W. Wei, Y. Zhu, J. Yang, and F. Yang, *Appl. Surf. Sci.* **301**, 539 (2014).
- <sup>46</sup>H. V. Jansen, M. J. de Boer, S. Unnikrishnan, M. C. Louwerse, and M. C. Elwenspoek, *J. Micromech. Microeng.* **19**, 033001 (2009).
- <sup>47</sup>C. J. Mogab, *J. Electrochem. Soc.* **124**, 1262 (1977).
- <sup>48</sup>H. Jansen, H. Gardeniers, M. de Boer, M. Elwenspoek, and J. Fluitman, *J. Micromech. Microeng.* **6**, 14 (1996).
- <sup>49</sup>H. Jansen, M. De Boer, H. Wensink, B. Kloock, and M. Elwenspoek, *Microelectron. J.* **32**, 769 (2001).
- <sup>50</sup>See: <https://www.americanelements.com/>.